

# Structural and functional characterisation of two proteolytic fragments of the bacterial protein toxin, pneumolysin

Peter J. Morgan<sup>a</sup>, Gayle Harrison<sup>a</sup>, Primrose P.E. Freestone<sup>a</sup>, Dennis Crane<sup>b</sup>,  
Arthur J. Rowe<sup>c</sup>, Timothy J. Mitchell<sup>1,a</sup>, Peter W. Andrew<sup>a</sup>, Robert J.C. Gilbert<sup>c,\*</sup>

<sup>a</sup>Department of Microbiology and Immunology, University of Leicester, Leicester, LE1 9HN, UK

<sup>b</sup>Laboratory of Molecular Structure, NIBSC, Blanche Lane, South Mimms, Potters Bar, Herts. EN6 3QG, UK

<sup>c</sup>NCMH, Department of Biochemistry, University of Leicester, Leicester, LE1 7RH, UK

Received 28 May 1997; revised version received 25 June 1997

**Abstract** Proteolytic cleavage of the bacterial protein toxin pneumolysin with protease K creates two fragments of 37 and 15 kDa. This paper describes the purification of these two fragments and their subsequent physical and biological characterisation. The larger fragment is directly involved in the cytolytic mechanism of this pore-forming protein, via membrane binding and self-association. The smaller fragment lacks ordered structure or discernible activity.

© 1997 Federation of European Biochemical Societies.

**Key words:** Pneumolysin; Domain structure and function; Analytical ultracentrifugation; Electron microscopy; Circular dichroism

## 1. Introduction

Pneumolysin is a 53-kDa pore-forming toxin produced by the Gram-positive bacterium *Streptococcus pneumoniae*. This bacterium is a major pathogen of man and causes pneumonia, meningitis and otitis media [1]. Pneumolysin has been shown to contribute to the virulence of the pneumococcus [2], and is consequently one of the pneumococcal proteins currently being studied as a protective antigen for use in an improved pneumococcal vaccine [3]. Pneumolysin is a member of a family of toxins referred to as the thiol-activated cytolysins, which are produced by four genera of Gram-positive bacteria. These toxins share a large number of structural characteristics and biological properties [4]. In addition, they may also share some common aspects in terms of their cytolytic mechanism with other water-soluble pore-forming proteins [5]. Pneumolysin has been extensively characterised [6–8], and is a useful model for studying the mechanism of pore formation by the thiol-activated toxins.

The mechanism of pore formation by the thiol-activated toxins is thought to involve several steps. Initially, the toxin interacts with the cell membrane (which must contain cholesterol), incorporates into the membrane and is then concentrated by lateral diffusion of toxin monomers in the membrane. The monomers undergo self-association to form large oligomeric structures, which appear on the surface of membranes as characteristic ring and arc-shapes.

In order better to understand the precise mechanism of the membrane incorporation and oligomerisation of thiol-activated toxins we have carried out a detailed structure/function study of pneumolysin. In the absence of a structure for pneumolysin we have attempted to assign functional domains to the protein and to characterise them. Previous studies with perfringolysin O (another of the thiol-activated toxins) have shown it to be susceptible to tryptic cleavage at a single site [9]. Single enzyme cleavage sites are often found in bacterial toxins [10] and tend to cleave them into functional domains. In common with perfringolysin O we have found that proteolytic cleavage of pneumolysin results in the production of a nicked derivative. This report describes the characterisation of the nicked toxin, along with that of the purified fragments generated from it. We have been able to assign functionality to the C-terminal fragment and suggest a possible role for the N-terminal fragment.

## 2. Materials and methods

### 2.1. Expression and purification of intact wild-type pneumolysin

Wild-type pneumolysin protein was expressed in *Escherichia coli* JM101, and purified as described previously [11]. Sample purity was checked by SDS-PAGE analysis, and haemolytic activity assayed as described previously [11].

### 2.2. Enzymatic cleavage and purification of nicked pneumolysin and fragments K1 and K2

Protease K (Sigma) was added to purified wild-type pneumolysin at a substrate:enzyme ratio of 20:1 (w/w). After 2 h incubation at room temperature the enzyme was inactivated with 5 mM phenylmethane-sulphonyl fluoride (Sigma). Protease K-cleaved pneumolysin was loaded onto a Mono Q 5/5 (Pharmacia) anion exchange column equilibrated in 20 mM Tris-HCl, pH 7.5. Pneumolysin fragments were separated from the intact toxin using an 18 ml linear gradient of 100 to 200 mM NaCl, at a flow rate of 0.5 ml min<sup>-1</sup>. Fractions containing the co-eluting fragments K1 and K2 were identified using SDS-PAGE, pooled, and incubated for 2 h at room temperature with 0.7 M sodium thiocyanate (see results). The dissociated fragments were then separated using a Superdex 75 (Pharmacia) gel permeation column equilibrated in 150 mM NaCl in 20 mM Tris-HCl, pH 7.5, at a flow rate of 0.33 ml min<sup>-1</sup>.

### 2.3. Analytical ultracentrifugation

Measurements were made using a Beckman Optima XL-A analytical ultracentrifuge. All samples were dialysed exhaustively against phosphate buffered saline (PBS; 8 mM Na<sub>2</sub>HPO<sub>4</sub>, 1.5 mM KH<sub>2</sub>PO<sub>4</sub>, 0.137 M NaCl, 2.5 mM KCl, pH 7.3) supplemented with varying concentrations of sodium thiocyanate (see Results). The solute distributions in the cell were recorded via their absorption at 278 nm. The low-speed sedimentation equilibrium method of ultracentrifugation was employed [12]. Multichannel, 'Yphantis-type' centrepieces [13] were used, enabling the simultaneous measurement of multiple samples. It was considered that equilibrium had been established when two consecutive scans, recorded several hours apart, were identical.

\*Corresponding author. Fax: (44) (116) 252 5260.  
E-mail: rjcg1@leicester.ac.uk

<sup>1</sup>Current address: Division of Infection and Immunity, Institute of Biomedical and Life Sciences, Joseph Black Building, University of Glasgow, Glasgow G12 8QQ, UK.

The final solute distribution data were captured and analysed using Beckman Origin software.

#### 2.4. Liposome binding assay

Liposomes were made by dissolving a mixture of phosphatidylcholine (10  $\mu\text{mol}$ ), cholesterol (10  $\mu\text{mol}$ ) and dicetylphosphate (1  $\mu\text{mol}$ ) in chloroform/methanol (1:1, v/v) and drying them under nitrogen [14]. The lipids were resuspended in PBS and dispersed by sonication in a sonic water bath for 90 seconds. The suspensions were then filtered through a 0.45  $\mu\text{m}$  filter (Millipore). To demonstrate binding ability, toxin samples were added to liposomes and incubated at 37°C for 60 min. These were then centrifuged for 6 min in a microfuge at 9500 $\times$ g. Supernatants and pellets were then analysed by electron microscopy and SDS-PAGE.

#### 2.5. Electron microscopy

Following vapour fixing for 1 min over glutaraldehyde solution, toxin samples were rinsed with distilled water and negatively stained, using either 0.8% (w/v) sodium phosphotungstate pH 6.8 or unbuffered 2% (w/v) uranyl acetate. All specimens were examined and photographed in a Siemens 102 transmission electron microscope, with the magnification calibrated using a diffraction grating replica.

#### 2.6. N-terminal sequencing

Pneumolysin peptides generated using protease K, were separated on a 15% SDS-PAGE gel, and electroblotted onto PVDF membranes (Immobilon P, Millipore) at 0–4°C in 25 mM Tris, 192 mM glycine, 0.037% (w/v) SDS and 10% (v/v) methanol. Blotted proteins were visualised with 0.1% (w/v) Coomassie Blue R-250 in (v/v) 50% methanol, followed by de-staining with 50% methanol (v/v) and 10% (v/v) acetic acid. N-terminal sequencing was performed on an Applied Biosystems 470A gas-phase sequencer.

#### 2.7. Circular dichroism and fluorescence spectroscopy

CD spectra were measured at 25.0°C using a Jasco J-720 spectropolarimeter using ammonium d-(+)-camphor-10-sulphonate as a reference standard. The sample was placed in a cell of path length 1.0 cm for near-UV (250–320 nm) and 0.05 cm for far-UV (190–250 nm). Molar ellipticities ( $[\theta]$ ) were determined using an  $A_{280}^{1\%}$  value of 13.6, calculated from the amino acid sequence and a molecular weight of 52 900 [15]. Secondary structure prediction was performed according to the Yang algorithm [16]. Each spectrum shown is the mean of 16 scans and has been corrected for solvent contribution by subtraction of a buffer blank.

Fluorescence spectra were recorded on a Spex Fluoromax single photon counting spectrofluorimeter. The bandwidth was 4.25 nm on both the excitation and emission monochromators. In each case the protein concentration has been adjusted to give an absorbance value at the excitation wavelength of approximately 0.05 in a 1.0 cm path-length cuvette. Spectra are the result of four scans normalised to a single protein concentration, with baselines subtracted.

### 3. Results

#### 3.1. Purification of nicked pneumolysin

Treatment of purified pneumolysin with protease K and subsequent purification by anion-exchange chromatography, resulted in the elution of two major peaks. SDS-PAGE analysis showed that one peak contained intact pneumolysin and the other contained two co-eluting fragments of pneumolysin (Fig. 1A). The smaller fragment (K1) had an apparent molecular weight of  $\sim$ 15 kDa and the larger fragment (K2)  $\sim$ 38 kDa. The fact that these two fragments of very different molecular weight co-elute under non-dissociating conditions, suggests that the proteolytic cleavage of pneumolysin at a single site results in the formation of a 'nicked' form of toxin, in which the two fragments produced remain physically associated. In order to confirm this suggestion, the weight average molecular mass of the 'nicked' pneumolysin was compared with that of the native protein by sedimentation equilibrium in the analytical ultracentrifuge. Values of  $M_w = 51\,000$  and

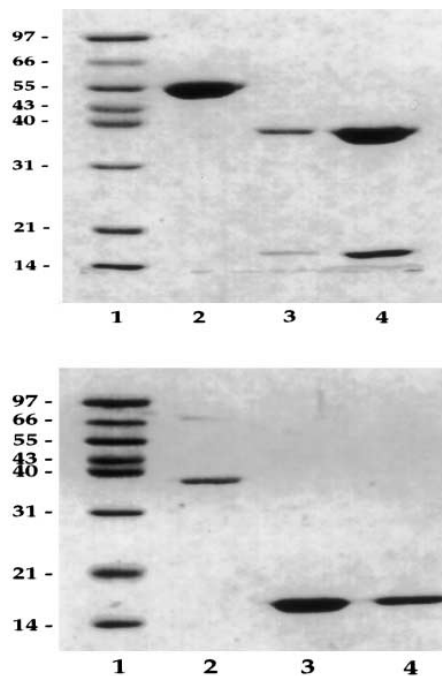


Fig. 1. (A) SDS-PAGE analysis of a preparation of pneumolysin treated with protease K which eluted in 2 separate peaks during anion-exchange chromatography showed that one peak contained intact pneumolysin (lane 2) and the other peak two fragments of pneumolysin (lanes 3 and 4) which co-eluted from the chromatography column. Lane 1 contains molecular weight markers. (B) SDS-PAGE analysis of nicked toxin treated with 0.7 M NaSCN and purified using gel permeation chromatography. Two peaks eluted, one of which contained purified 37-kDa fragment (K2) (lane 2) and the other the 15-kDa fragment (K1) (lanes 3 and 4). Lane 1 contains molecular weight markers.

$M_w = 52\,000$ , respectively, for the nicked and native protein, were determined. Within experimental error these are identical and may be compared with the value of  $M_w = 30\,700$ , which is the predicted average for a simple mixture of the two species. This confirms that the nicked species of pneumolysin remains essentially intact following proteolytic cleavage.

#### 3.2. Separation and purification of the fragments from nicked pneumolysin

In order to study the properties of the individual fragments it was necessary to separate them in a manner which caused as little perturbation to their secondary and tertiary structure as possible. However, agents which dissociate oligomeric proteins in general also have undesirable chaotropic effects. Sodium thiocyanate (NaSCN) is considered to be less chaotropic than other dissociating agents [17]. Thiocyanate is assumed to exert its dissociating properties by non-specific van der Waals binding to the surface of the protein molecules, thereby causing charge repulsion between them. The binding of  $\text{SCN}^-$  to a macromolecule can be predicted to have a Donnan type charge effect on the second virial coefficient. Hence, values estimated for  $M_w$  in the presence of thiocyanate will be too low by absolute standards, but should be a good guide as to the progress of dissociation. Addition of NaSCN to a final concentration of 0.5 to 0.7 molar resulted in a substantial fall in apparent  $M_w$  as determined by sedimentation equilibrium analytical ultracentrifugation, and higher concentrations pro-

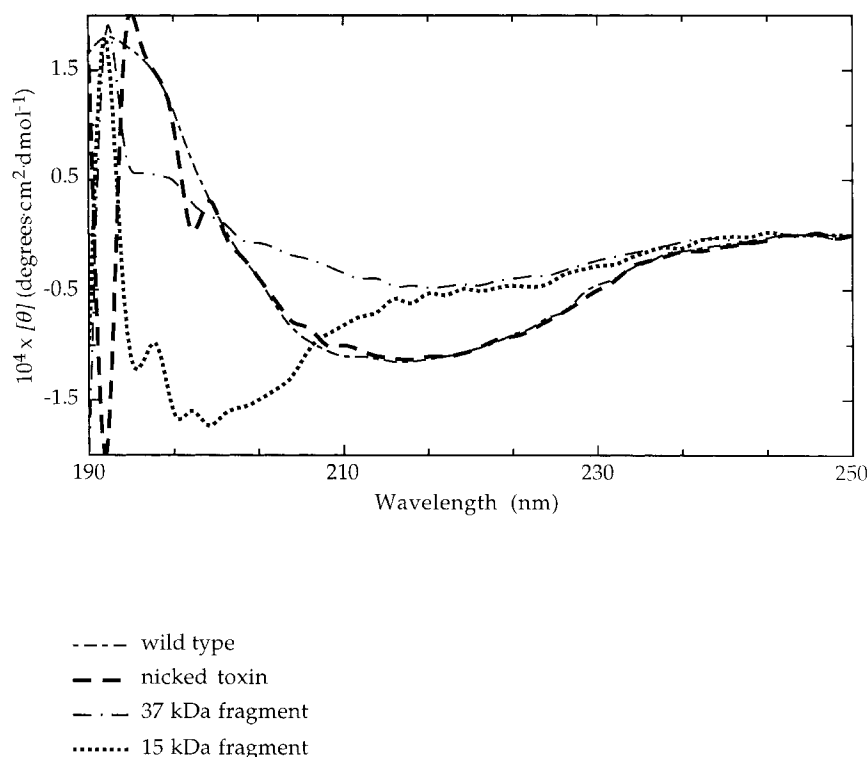


Fig. 2. Far-UV CD spectra of intact and nicked pneumolysin, and K2 and K1.

duced no further reduction. We therefore chose 0.7 M NaSCN as the optimal medium for separation of the nicked pneumolysin. After incubation for 4 h with thiocyanate, passage through a gel permeation column gave two well-resolved peaks. SDS-PAGE analysis (Fig. 1B) showed that one of these contained homogeneous 15-kDa fragment (K1) and the other the 37-kDa fragment (K2). N-terminal analysis of K1 gave the first 4 residues as alanine, asparagine, lysine, and alanine, which represents the N-terminal sequence of intact pneumolysin. The first four residues of K2 were asparagine, valine, proline, and alanine, corresponding to residues 143–146 of intact pneumolysin. Using this information we can assign mass values of 15 770 and 37 150 to K1 and K2, respectively, confirming the approximate size estimates determined by SDS-PAGE.

### 3.3. Spectroscopic analysis

The secondary and tertiary structure of nicked pneumolysin and its purified fragments were examined by circular dichroism (CD) and fluorescence spectroscopy. The data obtained for the 37-kDa fragment suffers from the presence of aggregate. In order to prevent self-association, the ionic strength of the buffer was raised, and this contributed to noise at around

195 nm. The RMS values for the fits obtained in calculating secondary structure composition were high as a result of these factors.

The far-UV CD spectrum of nicked pneumolysin is very similar to that of intact toxin (see Fig. 2) with an absorbance minimum at  $\sim 215$  nm. Secondary structure predictions for the nicked toxin based on the far-UV spectra (see Table 1) compare favourably to those reported previously for the intact toxin [6] (shown). A comparison of the near-UV spectra was also made (Fig. 3). Differences in intensity are seen in the 250–280 nm region between whole and nicked toxin. The fluorescence emission maxima of intact and nicked pneumolysin, excited at 295 nm, are shown in Table 1. While the emission spectra after excitation at 280 nm are essentially the same for both species of toxin, at 295 nm there was a significant loss of intensity in the emission spectrum of the nicked pneumolysin (data not shown). It seems therefore that although the two fragments remain associated, in the nicked toxin there is a change in the structure of the protein.

The far-UV spectra of fragments K1 and K2 are also shown in Fig. 2. The secondary structure prediction for K1 suggests some  $\beta$ -sheet and a high proportion of other structures (random coil, turn etc.) ( $\sim 60\%$ , see Table 1). The far-UV spec-

Table 1  
Biochemical and physical characteristics of pneumolysin and its proteolytic derivatives

	Sequence $M_w$	N-terminal sequence	Specific activity (HU/mg)	% $\alpha$ -helix <sup>a</sup>	% $\beta$ -sheet	% $\beta$ -turn	% other	$\lambda_{max}$ (excitation at 295 nm)
Intact pneumolysin	52 920	ANKA	$8.3 \times 10^5$	31	36	5	28	342
Nicked pneumolysin	52 920	ANKA	$4.5 \times 10^5$	20	58	0	22	346
37-kDa fragment	37 150	NVPA	0	13	65	0	22	337
15-kDa fragment	15 770	ANKA	0	0	39	0	61	347

<sup>a</sup>Secondary structure prediction was performed according to the Yang algorithm [15].

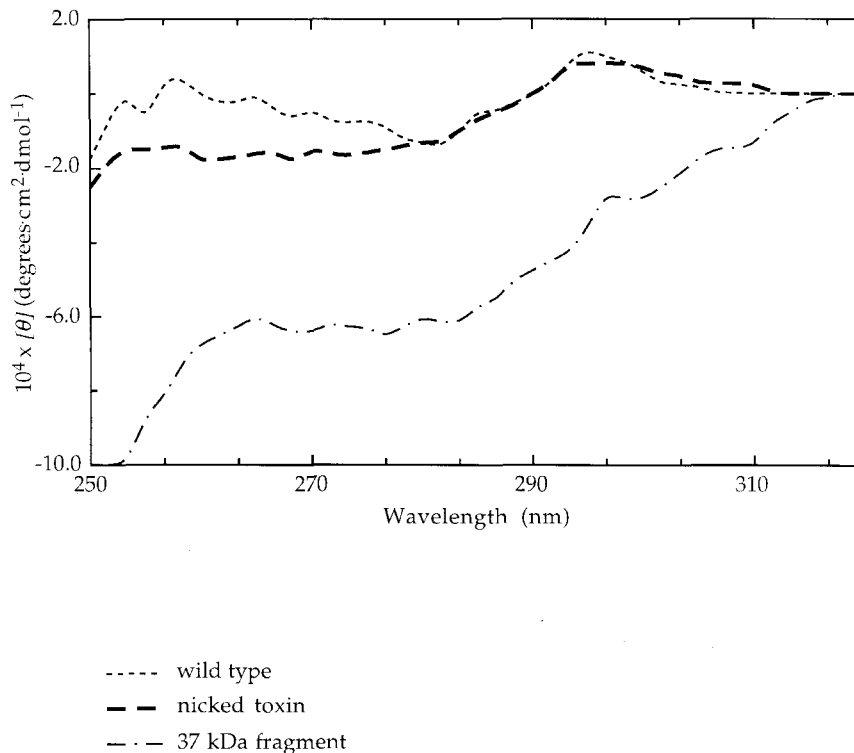


Fig. 3. Near-UV CD spectra of intact and nicked pneumolysin and K2.

trum for K2 predicts a large proportion of  $\beta$ -sheet (65%) and some  $\alpha$ -helix (13%). The near-UV spectrum of K2 (Fig. 3) was significantly different to the spectra of both intact and nicked pneumolysin. The local environment and interactions of some aromatic groups within the structure appear to have changed significantly. Unfortunately, sufficient material was not obtainable to allow the determination of a near-UV spectrum for K1. Fluorescence wavelength maxima for K1 and K2 excited at 295 nm are given in Table 1.

#### 3.4. Liposome binding and haemolytic activity

Binding to the liposomes was confirmed by electron microscopic observation of toxin that had interacted with, bound to and oligomerised on the liposomes. Images of negatively stained material from the intact and nicked pneumolysin (see Fig. 4A and B) showed typical oligomeric structures incorporated into liposomes. There were no such structures apparent in the images obtained with K1, either with or without liposomes. Liposomes which were incubated with K2 appeared to have protein incorporated into their surface (Fig. 4C). Whereas with intact pneumolysin arc and ring forms are seen (Fig. 4A), the oligomeric structures from K2 are predominantly arcs. Unlike nicked or native toxin, K2 sedimented from solution when centrifuged at  $9500 \times g$ .

No haemolytic activity was detected for either of the purified fragments, whereas the nicked toxin has a specific activity about half that of intact toxin (see Table 1). This may be a reflection of the differences seen in their secondary structures. Hence, although the 37-kDa fragment appears to oligomerize, the oligomers formed are non-functional – that is, they do not form pores. A mixture of purified K1 and K2 was also found to be non-haemolytic, showing that re-association to an active form does not occur.

#### 4. Discussion

Limited proteolysis of pneumolysin with the enzyme protease K resulted in a nicked derivative composed of two fragments; an N-terminal 15-kDa fragment (K1) and a C-terminal 37-kDa fragment (K2). Nicked toxin (in which the two fragments remain associated) was treated with sodium thiocyanate to enable the separation and subsequent purification of the individual fragments. Purified K2 has been shown by spectroscopic analysis to remain folded while K1 appeared to have lost its structure. Previous studies have described the production of nicked derivatives of perfringolysin [9], another of the thiol-activated toxins which has 48% sequence identity to pneumolysin. With perfringolysin, two alternative forms of nicked toxin were obtained by limited proteolysis with either subtilisin Carlsberg or trypsin. Interestingly, the cleavage site recognised in pneumolysin with protease K is in the same location as that recognised by subtilisin Carlsberg in perfringolysin. Protease K and subtilisin Carlsberg are both non-specific enzymes and are thought to cleave loop regions, which suggests that exposed loop regions are present at the cleavage site in both these proteins. The observation that enzymatic cleavage by a non-specific enzyme produces fragments of the same size in pneumolysin and perfringolysin presumably reflects their similar secondary/tertiary structure. The far-UV CD spectra of pneumolysin and perfringolysin [6,9,18,19] appear to substantiate this suggestion and predict the existence of a similarly high proportion of  $\beta$ -sheet. The near-UV CD spectra are also very similar suggesting that these proteins share a common tertiary structure.

The nicked toxin in which K1 and K2 remain associated has much the same conformation as wild type toxin and possesses haemolytic activity comparable to that of complete

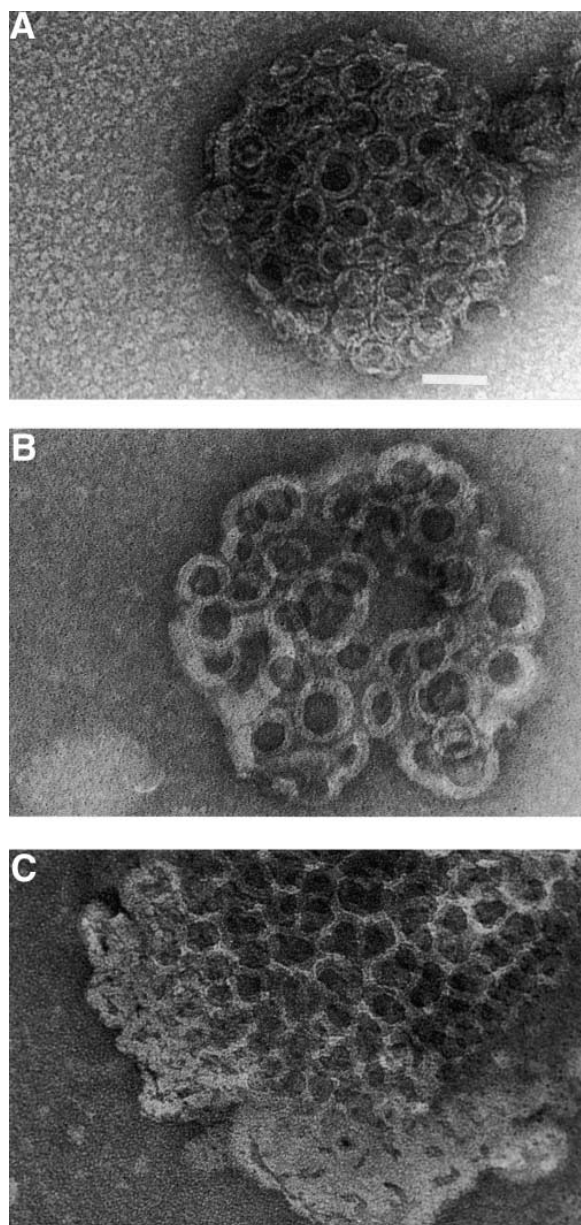


Fig. 4. Transmission electron microscope images of negatively-stained (A) intact pneumolysin, (B) 'nicked' pneumolysin and (C) K2, all of which have been incubated with liposomes. Bar indicates 50 nm.

pneumolysin. The oligomers formed by it were observed by electron microscopy to be similar to those formed by intact pneumolysin. While K2 remained capable of cell-binding and oligomerization (although the oligomers formed were non-conducting), K1 lacked any activity.

That the C-terminal fragment, with its domain structure still largely complete, can bind and self-associate strongly indicates that it fulfils these two functions in complete pneumolysin. This compares favourably with previous data obtained by us indicating that C-terminal deletions from pneumolysin [20] and antibodies whose epitopes lie in the C-terminal region [21] inhibit its binding activity while mutation of particular

residues within the sequence of K2 away from the C-terminus inhibit pore-formation [22]. Similar mutational results have been obtained in streptolysin O (another thiol-activated toxin) by Palmer and co-workers [23,24], and in perfringolysin O the C-terminal fragment generated using subtilisin Carlsberg also has similar structural and functional attributes [19]. Although no activity has been demonstrated for the N-terminal fragment K1 due to its denaturation consequent upon separation from K2, the fact that K2 lacks haemolytic activity and fails to form complete rings in the manner of whole and nicked pneumolysin indicates a role for K1 in maintaining the structure and therefore function of the protein.

## References

- [1] Austrian, R. (1981) *Rev. Infect. Dis.* 3, 183–189.
- [2] Berry, A.M., Yother, J., Briles, D.E., Hansman, D. and Paton, J.C. (1989) *Infect. Immun.* 57, 2037–2042.
- [3] Andrew, P.W., Boulnois, G.J., Mitchell, T.J., Lee, C.-J., Paton, J.C., Poolman, J.T. and Peeters, C.C.A.M. (1994), in: *Bacterial Protein Toxins* (J.H. Freer et al., Eds.), pp. 453–466, Gustav Fischer Verlag, Stuttgart.
- [4] Alouf, J.E. and Geoffroy, C. (1991), in: *Sourcebook of Bacterial Protein Toxins* (J.E. Alouf and J.H. Freer, Eds.), pp. 147–186, Academic Press, London.
- [5] Bhakdi, S., Bayley, H., Valeva, A., Walev, I., Walker, B., Weller, U., Kehoe, M. and Palmer, M. (1996) *Arch. Microbiol.* 165, 73–79.
- [6] Morgan, P.J., Varley, P.G., Rowe, A.J., Andrew, P.W. and Mitchell, T.J. (1993) *Biochem. J.* 296, 671–674.
- [7] Morgan, P.J., Hyman, S.C., Byron, O., Andrew, P.W., Mitchell, T.J. and Rowe, A.J. (1994) *J. Biol. Chem.* 269, 25315–25320.
- [8] Morgan, P.J., Hyman, S.C., Rowe, A.J., Mitchell, T.J., Andrew, P.W. and Saibil, H.R. (1995) *FEBS Lett.* 371, 77–80.
- [9] Ohno-Iwashita, Y., Iwamoto, M., Mitsui, K.-i., Kawasaki, H. and Ando, S. (1986) *Biochemistry* 25, 6048–6053.
- [10] Tweten, R.K., Harris, R.W. and Sims, P.J. (1991) *J. Biol. Chem.* 266, 12449–12454.
- [11] Mitchell, T.J., Walker, J.A., Saunders, F.K., Andrew, P.W. and Boulnois, G.J. (1989) *Biochim. Biophys. Acta* 1007, 67–72.
- [12] Creeth, J.M. and Pain, R.H. (1967) *Prog. Biophys. Mol. Biol.* 17, 217–287.
- [13] Yphantis, D.A. (1964) *Biochemistry* 3, 297–317.
- [14] Cowell, J.L., Kim, K. and Bernheimer, A. (1978) *Biochim. Biophys. Acta* 507, 230–241.
- [15] Walker, J.A., Allen, R.L., Falmagne, P., Johnson, M.K. and Boulnois, G.J. (1987) *Infect. Immun.* 55, 1184–1189.
- [16] Yang, J.T., Wu, C.S.C. and Martinez, H.M. (1986) *Methods Enzymol.* 130, 208–269.
- [17] Djaballah, H., Rowe, A.J., Harding, S.E. and Rivett, A.J. (1993) *Biochem. J.* 292, 857–862.
- [18] Nakamura, M., Sekino, N., Iwamoto, M. and Ohno-Iwashita, Y. (1995) *Biochemistry* 34, 6513–6520.
- [19] Iwamoto, M., Ohno-Iwashita, Y. and Ando, S. (1990) *Eur. J. Biochem.* 194, 25–31.
- [20] Owen, R.H.G., Boulnois, G.J., Andrew, P.W. and Mitchell, T.J. (1994) *FEMS Microbiol. Lett.* 121, 217–222.
- [21] de los Toyos, J.R., Méndez, F.J., Aparicio, J.F., Vázquez, F., del Mar García Suárez, M.M.G., Fleites, A., Hardisson, C., Morgan, P.J., Andrew, P.W. and Mitchell, T.J. (1996) *Infect. Immun.* 64, 480–484.
- [22] Pasternak, C.A., Alder, G.M., Bashford, C.L., Korchev, Y.E., Pederzoli, C. and Rostovtseva, T.K. (1992) *FEMS Microbiol. Immunol.* 105, 83–92.
- [23] Palmer, M., Valeva, A., Kehoe, M. and Bhakdi, S. (1995) *Eur. J. Biochem.* 231, 388–395.
- [24] Palmer, M., Saweljew, P., Vulicevic, I., Valeva, A., Kenoe, M. and Bhakdi, S. (1996) *J. Biol. Chem.* 271, 26664–26667.